Computational and Structural Biotechnology Journal 23 (2024) 1051–1064

Contents lists available at ScienceDirect

Computational and Structural Biotechnology Journal

journal homepage: www.elsevier.com/locate/csbj

Research article

Uncovering the potential of APOD as a biomarker in gastric cancer: A retrospective and multi-center study

Zisong Wang [a,b], Hongshan Chen [a], Le Sun [c], Xuanyu Wang [c], Yihang Xu [a], Sufang Tian [a,*], Xiaoping Liu [a,*]

[a] Department of Pathology, Zhongnan Hospital of Wuhan University, Wuhan 430071, Hubei Province, China
[b] School of Basic Medical Sciences, Wuhan University, Wuhan 430071, Hubei Province, China
[c] Department of Urology, Zhongnan Hospital of Wuhan University, Wuhan 430071, Hubei Province, China

ARTICLE INFO

Keywords:
Gastric cancer
APOD
Cancer biomarker
Tumor microenvironment
Immunotherapy

ABSTRACT

Gastric cancer (GC) poses a significant health challenge worldwide, necessitating the identification of predictive biomarkers to improve prognosis. Dysregulated lipid metabolism is a well-recognized hallmark of tumorigenesis, prompting investigation into apolipoproteins (APOs). In this study, we focused on apolipoprotein D (APOD) following comprehensive analyses of APOs in pan-cancer. Utilizing data from the TCGA-STAD and GSE62254 cohorts, we elucidated associations between APOD expression and multiple facets of GC, including prognosis, tumor microenvironment (TME), cancer biomarkers, mutations, and immunotherapy response, and identified potential anti-GC drugs. Single-cell analyses and immunohistochemical staining confirmed APOD expression in fibroblasts within the GC microenvironment. Additionally, we independently validated the prognostic significance of APOD in the ZN-GC cohort. Our comprehensive analyses revealed that high APOD expression in GC patients was notably associated with unfavorable clinical outcomes, reduced microsatellite instability and tumor mutation burden, alterations in the TME, and diminished response to immunotherapy. These findings provide valuable insights into the potential prognostic and therapeutic implications of APOD in GC.

1. Introduction

Gastric cancer (GC) represents a highly heterogeneous malignancy at the molecular, tissue, and immune microenvironment levels, ranking fifth and third in incidence and mortality, respectively, among all cancers [1]. For patients with early-stage GC, surgical resection of the tumor is the primary treatment, and the corresponding prognosis is relatively good. However, the early symptoms of GC are often atypical, leading to diagnosis at advanced stages where surgical radical treatment is no longer feasible, resulting in a median overall survival (OS) limited to 12 months [2]. While surgical treatment can significantly improve survival rates, postoperative recurrence is common, leading to a poor prognosis for patients upon GC recurrence [3]. Recently, the introduction of new approaches including human epidermal growth factor receptor 2 (HER2) inhibitors and vascular endothelial growth factor receptor 2 (VEGFR2) inhibitors in combination with chemotherapy, has substantially improved the long-term survival of GC patients. However, drug resistance and side effects of chemotherapy remain a challenge for GC patients [4]. Consequently, developing novel biomarkers for early GC screening, predicting therapy response, detecting disease recurrence, and assessing OS is crucial for enhancing clinical outcomes and extending survival.

High-throughput sequencing technologies have revolutionized various clinical and biomedical research fields, including studies on malignant tumors [5]. These technologies have significantly enhanced the capability to investigate the causes, pathogenesis, progression, and targeted therapies of various diseases [6].

Human apolipoproteins (APOs), comprising 22 members consisting

Abbreviations: APOD, apolipoprotein D; APOs, apolipoproteins; CAF, cancer-associated fibroblast; CNV, copy number variation; CoxPH, Cox proportional hazards regression model; DEGs, differentially expressed genes; GC, gastric cancer; GEO, Gene Expression Omnibus; GO, Gene Ontology; GSEA, Gene Set Enrichment Analysis; GSVA, Gene Set Variation Analysis; IHC, immunohistochemistry; KEGG, Kyoto Encyclopedia of Genes and Genomes; KM, Kaplan-Meier; MSI, microsatellite instability; OS, overall survival; RMST, restricted mean survival time; RNA-Seq, RNA sequencing; ssGSEA, single sample gene set enrichment analysis; TCGA, The Cancer Genome Atlas; TMB, tumor mutation burden; TME, tumor microenvironment.

* Corresponding authors at: Department of Pathology, Zhongnan Hospital of Wuhan University, Wuhan 430071, Hubei Province, China.
E-mail addresses: sftian@whu.edu.cn (S. Tian), liuxiaoping@whu.edu.cn (X. Liu).

https://doi.org/10.1016/j.csbj.2024.02.015
Received 21 October 2023; Received in revised form 16 February 2024; Accepted 16 February 2024
Available online 24 February 2024

of APOA1, APOA2, APOA4, APOA5, APOB-48, APOB-100, APOC1, APOC2, APOC3, APOC4, APOD, APOE, APOH, APOL1, APOL2, APOL3, APOL4, APOL5, APOL6, APOM, APOO, and APOJ, play critical roles in lipid metabolism and inflammatory responses [7]. Studies have shown that APOs are associated with GC prognosis. For instance, the ratio of preoperative serum APOB to APOA1 has been used as a prognostic indicator for GC [8], and tumor-associated macrophage-derived exosomes promote migration of GC cells through the transfer of functional APOE [9]. Therefore, APOs represent promising targets and markers for tumor treatment and prevention.

Apolipoprotein D (APOD), a 25–30 kDa glycosylated protein belonging to the APO family, has multifunctional roles in lipid transport, food intake, inflammation, antioxidant response, and development, and is implicated in several cancers [10]. Previous research indicates that increased levels of tumor APOD expression are associated with poor clinical outcomes in breast cancer patients[11]. In hepatocellular carcinoma tissues, APOD expression is significantly downregulated compared to that in the corresponding normal tissues and serves as an independent predictive biomarker [12]. Similarly, in colorectal tumors, APOD expression is significantly downregulated and correlated with advanced stage, lymphatic metastasis, and worse OS [13]. However, in malignant melanoma, APOD is highly expressed and may be a prognostic marker [14]. However, the characteristics and roles of APOD in GC remain elusive, warranting further investigation of its potential as a biomarker for GC diagnosis, prognosis, and management.

In the present study, we comprehensively investigated the characteristics of APOs at the pan-cancer level, examined the immune profiles of APOD in pan-cancer and its associations with genomic heterogeneity, and finally, systematically evaluated the correlations between APOD and GC and validated the findings in independent cohorts. Our results indicated that APOs, particularly APOD, was significantly associated with various cancers, including GC. Moreover, APOD emerged as a potential independent prognostic factor and therapeutic target for GC, providing novel avenues for its clinical management.

2. Material and methods

2.1. GC gene expression studies

The Cancer Genome Atlas (TCGA) pan-cancer RNA sequencing (RNA-Seq) data in transcripts per million (TPM) values, clinical information, and gene-level copy number variation (CNV) assessed using GISTIC2 were obtained from UCSC Xena (https://xenabrowser.net/) [15]. The somatic mutation annotation file (MAF) for GC was obtained through the R package “TCGAmutations” [16]. A total of 348 GC samples from TCGA-STAD project [17] and 300 samples from the Gene Expression Omnibus (GEO) dataset GSE62254 [18] were obtained from the R package “CuratedCancerPrognosisData” [19].

2.2. Exploring the pan-cancer characteristics of APOs

We initially calculated the expression patterns of APO family between tumor tissues and adjacent normal controls in the pan-cancer atlas from TCGA, represented as log2(Fold Change). Subsequently, we utilized the univariate Cox proportional hazards regression models (CoxPHs) to estimate the survival relevance of the expression levels of APOs in each cancer type. Furthermore, we employed the Gene Set Cancer Analysis (GSCA) platform [20] to assess the associations between the Gene Set Variation Analysis (GSVA) scores of APOs and levels of immune infiltration, as well as the associations between APOs and subtypes of nine cancers (HNSC, LUSC, COAD, STAD, LUAD, GBM, BRCA, KIRC, BLCA) using data from TCGA. Additionally, using pan-cancer RNA-seq and CNV data in TCGA, we calculated the amplification and deletion rates of APOs in pan-cancer, with a threshold of 0.05. Finally, we constructed the protein-protein interaction network of APOs using the STRING database (Version 11.5) (https://string-db.org/).

2.3. Investigating the pan-cancer characteristics of APOD

The expression profiles of APOD were obtained from the Pan-Cancer dataset of TCGA. High-quality prognostic data, retrieved from previous studies [21], was used after excluding samples with a follow-up time less than 30 days. CoxPHs were applied to evaluate the prognostic correlations between APOD expression and the OS of patients at pan-cancer level, with significance evaluated using Log-rank tests. Wilcoxon Rank Sum and Signed Rank Tests were employed for unpaired analyses of differences of APOD expression among different T stages and grades in each tumor, and Kruskal-Wallis tests were used for multi-group comparisons. We retrieved the level 4 single-nucleotide variant data of all samples in the TCGA project preprocessed by MuTect2 [22] from GDC (https://portal.gdc.cancer.gov/), integrated the mutation data of the samples, used the R package "maftools" [23] to obtain the structural domain information of the proteins, and plotted the lollipop plot of APOD mutations in pan-cancer. We applied the "Immune" module of TIMER2.0 [24] that integrates multiple approaches for estimating tumor immune microenvironment to evaluate the associations between APOD expression in pan-cancer and the infiltration levels of 19 immune cell types using Spearman’s correlations. In addition, we integrated pan-cancer APOD expression data with microsatellite instability (MSI) [25], purity [26], and tumor mutation burden (TMB) scores of samples, and calculated the Spearman’s correlations between APOD expression and these three scores in different types of cancers. We also extracted 150 marker genes of immune pathways, including chemokines, receptors, MHCs, immunoinhibitors and immunostimulators, from the TISIDB database [27], and calculated the Spearman’s correlations between APOD expression and these immune-regulatory genes at pan-cancer level using the Sangerbox platform [28]. Subsequently, we further utilized the R package "ESTIMATE" [29] to estimate the stromal score, immune score, and ESTIMATE score of each patient in each tumor based on the gene expression profiles, and calculated the Spearman’s correlations between APOD expression and these three scores.

2.4. Characterization of the correlation between APOD expression and clinicopathological information of patients with GC

Firstly, we divided GC patients into high and low APOD expression groups based on the median of APOD expression level. Using R package "table1", we compared the differences between patients in different groups in terms of age, gender, pathological classification, grade, stage, etc. Additionally, Kaplan-Meier (KM) curve analysis was applied to evaluate the survival differences between high and low APOD expression groups, and then the restricted mean survival time (RMST) was calculated and estimated between the two groups. We then used stepwise regressions to select the most relevant variables and performed both univariate and multivariate CoxPHs based on APOD expression groups and clinicopathologic information. Based on the inclusion of variables in the CoxPHs, we calculated the concordance indexes (C-indexes) with and without APOD expression groups, and compared the two. To increase the reliability of our results, we divided the TCGA-STAD and GSE62254 cohorts into three groups based on APOD expression tertiles for trend analysis. We selected the median value of each group as the representative value, included APOD grouping, survival status and follow-up time in models, and calculated the p-value for trend of each cohort. We further utilized KM curves to visually demonstrate the prognostic characteristics of the tertile groups.

2.5. Investigating the possible functions of APOD in GC

Differentially expressed genes (DEGs) between different expression groups of APOD were identified using the R package "DESeq2" in TCGA-STAD. We considered genes with $|\log2(FC)| > 2$ and an adjusted p-value

< 0.05 as significant DEGs. Based on the DEGs, we performed Gene Ontology (GO) analysis, Kyoto Encyclopedia of Genes and Genomes (KEGG) analysis, and Gene Set Enrichment Analysis (GSEA). For the GSEA, we employed the c5.all.v7.0.entrez.gmt dataset from the MSigDB database, utilizing the R package "clusterProfiler". A p-value < 0.05 from Fisher's test was considered indicative of significance.

2.6. Investigating the relationship between APOD expression and GC tumor microenvironment (TME)

We employed multiple algorithms to assess the relationship between APOD expression and TME in GC. Firstly, we downloaded the 22 immune cell subtypes (LM22) files and estimated the infiltration levels of these immune cells in GC based on the R CIBERSORT script (Version 1.03) [30]. Next, we used the R "ESTIMATE" package to calculate stromal, immune and ESTIMATE scores. Finally, we utilized the R package "ConsensusTME" [31] to estimate the contribution of 18 immune cell types to the GC TME and performed Wilcoxon tests to compare infiltration levels between different groups.

2.7. Exploring the correlations between APOD expression and cancer biomarkers

We systematically collected biomarkers related to cancer, including IFN-γ signature [32], onco-pathways [33], metabolism pathways [34], and cancer hallmark pathways [35]. In addition, we also collected key genes for lipid metabolism from previous study [36]. Then, we applied single sample gene set enrichment analysis (ssGSEA) using the R package "GSVA" to obtain scores for each sample based on the expression matrices of TCGA-STAD and GSE62254. Finally, we explored the correlations between the expression of APOD and these biomarkers.

2.8. Exploring the correlations between APOD expression and GC tumor mutations and immune therapy

Somatic mutation data of TCGA-STAD were downloaded from the R package "TCGAmutations" and the TMB for each sample was calculated using the R package "maftools". Additionally, we used the Tumor Immune Dysfunction and Exclusion (TIDE) database to predict the responsiveness of TCGA-STAD and GSE62254 samples to immune checkpoint inhibitors [37] with gene expression data standardized according to the requirements. Subsequently, TIDE scores were obtained for each sample. In addition, we compared the levels of APOD expression in two groups, the immunotherapy responsive and non-responsive groups, consisting of 45 metastatic GC samples treated with the PD-1 inhibitor pembrolizumab [38], with normalized RNA-seq data obtained from the TIDE database.

2.9. Expression of APOD in single cells

Using the TISCH2 database [39], we analyzed the cell clustering patterns in two single-cell datasets, GSE134520 [40] and GSE167297 [41], and investigated the expression patterns of APOD in single cells, as well as the relationships among different cell clusters.

2.10. Exploring the association of APOD with drug treatment in GC patients

We utilized the CellMiner database [42] to obtain processed RNA expression data and drug data (DTP NCI-60) for further analysis. For the drug data, we imputed missing values using the R package "impute" with K-nearest neighbor (KNN) method. In addition, we also employed the R package "pRRophetic" [43] to construct ridge regression models using gene expression profiles from the Genomics of Drug Sensitivity in Cancer (GDSC) database and RNA-seq data from TCGA-STAD and GSE62254 to predict drug IC50 values. Afterwards, Spearman's correlations were used to assess the associations between APOD expression and different drugs.

2.11. Investigation of the interactions between APOD and other proteins

We used the ComPPI database (Version 2.1.1) to retrieve the interactome of human APOD protein with other proteins [44]. We extracted six types of targets, including Cytosol, Secretory-pathway, Extracellular, Membrane, Mitochondrion, and Nucleus. Subsequently, we calculated interaction scores using the formulas provided at the website (http://comppi.linkgroup.hu/help/scores). Finally, we visualized the protein-protein interaction network using the R package "igraph".

2.12. Tissue microarray constructing and immunohistochemistry (IHC) staining

We retrospectively collected 108 samples of patients with GC and their corresponding clinicopathological information from the Zhongnan Hospital of Wuhan University, which were named ZN-GC cohort, under Institutional Review Board approval (2020133) with a waiver of informed consent. A tissue microarray was constructed using the GC samples we collected. The tissue microarray was baked at 75 °C for 2 h, then deparaffinized and rehydrated, followed by high-pressure cooking with EDTA for 2.5 min, incubated with hydrogen peroxide at room temperature for 10 min, and then rinsed with PBS. The microarray was blocked with goat serum for 1 h, and then washed with PBS. APOD primary antibody (1:150, Proteintech) was added and incubated overnight at 4 °C. The microarray was then taken out, reheated, and secondary antibody was added and incubated at room temperature for 40 min, followed by PBS rinsing. DAB staining was performed, and then the microarray was counterstained with hematoxylin, dehydrated with ethanol and air-dried before sealing the slides. We utilized the Hamamatsu NanoZoomer XR slide scanner to scan corresponding 40 × magnification tissue microarray images. Afterwards, we employed QuPath-0.4.3 [45] to recognize images and measure positively stained cells. We classified the patients into high and low expression groups according to the median of APOD positivity rates, used R package "table1" to analyze the clinicopathological information of the patients, and then used KM curves, RMST, univariate and multivariate CoxPHs, and C-indexes with and without APOD to validate the prognostic role of APOD. We also conducted staining for α-SMA, a marker of fibroblasts, and compared the results with APOD staining at the same tissue location to investigate the relationship between APOD expression and fibroblasts.

2.13. Statistical analysis

All statistical analyses and plotting were performed in R software (Version 4.2.1, https://www.r-project.org/). Wilcoxon test was used for comparisons between two groups, while Kruskal-Wallis test was used for comparisons among multiple groups. Spearman's correlation was used for correlation analysis. Chi-square analysis was used to reveal clinicopathological information of patients. Survival curves were plotted using the KM method, and differences in OS were analyzed using Log-rank tests and RMST method. Univariate and multivariate CoxPHs were constructed to characterize the prognostic roles of genes, with 95% confidence intervals (CI). A p-value < 0.05 was considered statistically significant (* $p < 0.05$, ** $p < 0.01$, *** $p < 0.001$).

3. Results

3.1. Differential expression of APOs in pan-cancer and their associations with clinical features

To investigate the expression patterns of APOs in pan-cancer, we utilized the pan-cancer data from TCGA to calculate the differential

expressions of APOs between tumor tissues and adjacent normal tissues. The heatmap analysis revealed varying expression levels of APOs, with genes such as APOA1, APOD, and APOH commonly downregulated across most cancers, while others like APOC1 and APOC2 exhibited upregulation in many cancers. Even within the same cancer type, such as COAD, KICH, and STAD, the expression trends of APOs varied considerably (Fig. 1A). Subsequently, we performed CoxPHs to analyze the relationships between APOs expressions and pan-cancer prognosis, and the results showed that there was a highly variable impacts of APOs expressions on prognosis in pan-cancer was also highly variable, with the effect of a particular gene on prognosis being opposite in different tumors (Fig. 1B). Additionally, correlation analyses identified significant associations between specific APOs and distinct cancer subtypes, including STAD, LUAD, BRCA, KIRC, LUSC, and GBM (Supplementary Figure 1A).

3.2. The relationships between APOs and TME and CNV, and construction of APOs protein interaction network

To evaluate the associations between APOs expression and pan-cancer immune infiltration, we calculated the GSVA scores of APOs and generated a heatmap to show the correlations between GSVA scores of APOs and pan-cancer immune infiltration indicators. Our analysis revealed that immune cells such as dendritic cells (DC) and natural killer (NK) cells were positively correlated with GSVA scores in most cancers, while neutrophils showed a negative correlation. Particularly, in almost all cancers, GSVA scores of APOs showed a significant positive correlation with overall immune infiltration levels, suggesting active participation of APOs in the TME (Fig. 1C). Further investigation into CNV can provide insights into the composition of the tumor genome, inter-individual genetic differences, and genetic pathogenic factors. Therefore, we examined the CNV percentages of APOs in pan-cancer, and the results showed that APOD, APOA2 and APOH were more likely to be amplified, while APOA1, APOC3, APOA5 and APOL5 were more likely to be deleted in pan-cancer (Fig. 1D). Finally, we leveraged the STRING database to construct a comprehensive protein-protein interaction network for APOs (Supplementary Figure 1B). This network provides a valuable resource for exploring downstream functional interactions and regulatory pathways involving APOs.

3.3. Prognostic, immunological, tumor heterogeneity and mutation features of APOD in Pan-Cancer

Our findings identified significant characteristics of APOD among APOs in pan-cancer, including its expression, prognostic role, immune infiltration, and CNV patterns. To further explore its intricacies, we investigated the characteristics of APOD in various cancers. We found that high expression of APOD was associated with poor prognosis in six tumor types (STAD, STES, KIPAN, COADREAD, THCA, READ), while low expression of APOD was associated with poor prognosis in six tumor types (GBMLGG, BRCA, THYM, MESO, SKCM-M, SKCM) (Supplementary Figure 2). Pathological stage can evaluate the severity and extent of tumors. Based on integrated data of APOD expression and tumor stage information in pan-cancer, we found that APOD expression was significantly correlated with pathological stages in various cancers. For example, in STAD, the expression of APOD gradually increased with the progression of the T stages and the grades (Supplementary Figure 3 A, B). By integrating mutation data and protein structural domain information, we found that APOD had a high incidence of missense mutations in the structural domains of 189aa and particularly Lipocalin in various cancers (Supplementary Figure 3 C). Through analyses of 150 immune-related genes categorized as chemokines, receptors, MHC, immunoinhibitors, and immunostimulators, we found significant correlations between APOD expression and various immune regulators in pan-cancer (Supplementary Figure 4 A). Additionally, we utilized the TIMER 2.0 database with multiple algorithms to calculate the correlations between APOD expression and immune cell infiltration levels in pan-cancer. The results showed that APOD expression was positively associated with cancer-associated fibroblasts (CAFs), endothelial cells and hematopoietic stem cells in most cancers, while negatively correlated with myeloid-derived suppressor cells (MDSCs), suggesting that APOD played a role in the process of immune infiltration in pan-cancer (Fig. 2A). Subsequently, we used the ESTIMATE algorithm to evaluate the relationship between APOD expression and TME in pan-cancer. The results of stromal scores, immune scores, and ESTIMATE scores suggested an association between APOD and the TME of various tumors (Supplementary Figure 4B-D). Due to the potential impact of tumor heterogeneity on various factors such as tumor growth rate, invasiveness, drug sensitivity, prognosis, etc., we evaluated three indicators of tumor heterogeneity, including MSI, purity, and TMB. We found that the trend of APOD expression with these three indicators was not consistent in different cancers. Specifically, the expression of APOD showed a strongly negative correlation with MSI, purity, and TMB in GC (Fig. 2B).

3.4. APOD indicates poor prognosis in GC patients

Our pan-cancer analysis identified APOD as a detrimental prognostic biomarker in GC patients, associated with the GC microenvironment. APOD expression displayed a significantly negative correlation with MSI, purity, and TMB in GC, prompting us to delve deeper into its role in this specific cancer. First, we analyzed clinicopathologic data of GC patients in TCGA-STAD and GSE62254 (Supplementary Table 1, 2). Consistent with our initial findings, high APOD expression correlated with shorter OS time, supported by KM curves and confirmed by RMST analyses (Fig. 3A, C & Supplementary Table 3, 4). By employing univariate and multivariate CoxPHs, we further confirmed that High APOD expression was an independent prognostic risk factor for GC patients (Fig. 3B, D). To investigate the contribution of APOD to the prognostic model, we compared models with and without APOD expression groups. The models including APOD demonstrated higher C-indexes compared to the models without APOD, suggesting that APOD expression improved the predictive performance of the models and that APOD played an important role in GC prognosis (Supplementary Figure 5 A, B). To strengthen our findings, we divided TCGA-STAD and GSE62254 into three groups based on APOD expression tertiles. Including APOD grouping, survival status, and follow-up time in the model, we calculated a p-value for trend of 0.013 in TCGA-STAD and $4.65 \times 10–6$ in GSE62254, confirming a significant correlation between APOD expression and patient survival. KM curves stratified by APOD expression tertiles further illustrated that patients with high APOD expression had a worse prognosis (Supplementary Figure 5D, E).

3.5. APOD participates in multiple biological functions in GC and is associated with TME

To investigate the potential functions of APOD in GC, we performed enrichment analyses on DEGs between high and low APOD expression groups in TCGA-STAD. We conducted GO enrichment analysis to explore the cellular component (CC), molecular function (MF) and biological process (BP) that APOD might be involved in, and the results revealed associations with myofibril, metal ion transmembrane transporter activity, muscle cell development, etc. (Fig. 3E & Supplementary Table 5). KEGG pathway enrichment analysis suggested that APOD was primarily enriched in protein digestion and absorption, chemical carcinogenesis - receptor activation and other signaling pathways (Fig. 3F & Supplementary Table 6). GSEA based on the MsigDB database revealed significant enrichment of APOD in actomyosin structure organization, regulation of hormone secretion and other functions (Supplementary Figure 6 A). Collectively, the results of the three enrichment analyses suggested that APOD might be involved in ion transport, digestion and absorption, secretion, hormone regulation, and other signaling pathways in GC. The TME plays a crucial role in tumor initiation and

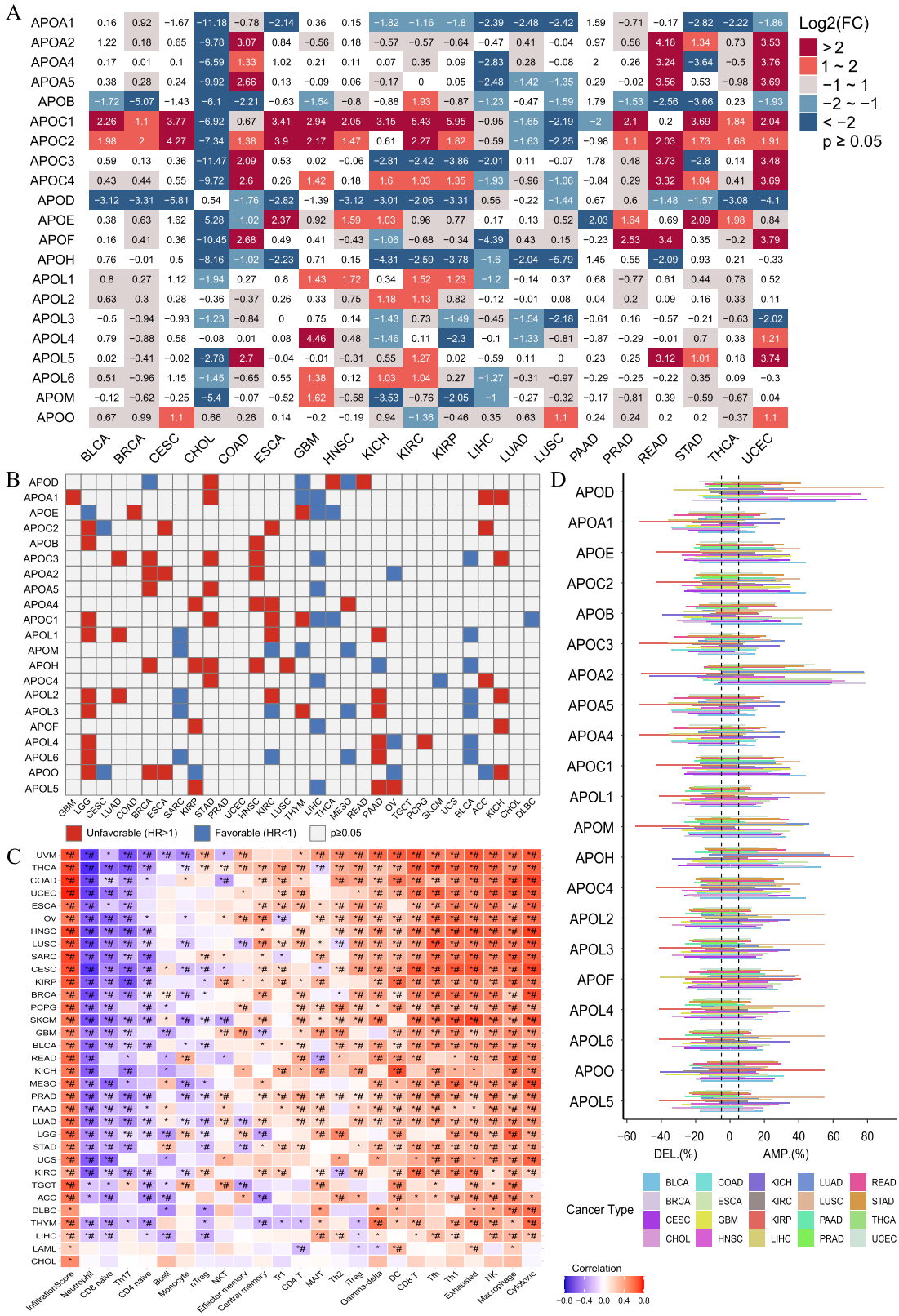

Fig. 1. The pan-cancer analyses of APOs. (A) Expression trends of APOs in pan-cancer, where FC represents the fold change in gene expressions relative to normal in tumor samples. The white color filling indicates a p-value > 0.05. (B) CoxPHs were employed to calculate the associations between gene expressions and prognosis, where HR> 1 represents an unfavorable association, HR< 1 indicates a favorable association, and the remaining are those with p-values > 0.05. (C) Correlations between the GSVA scores of APOs and immune infiltration indicators (*: P value ≤ 0.05; #: FDR ≤ 0.05). (D) Amplification and deletion rates of APOs in pan-cancer, calculated using CNV data (the threshold for amplification and deletion was set at 0.05).

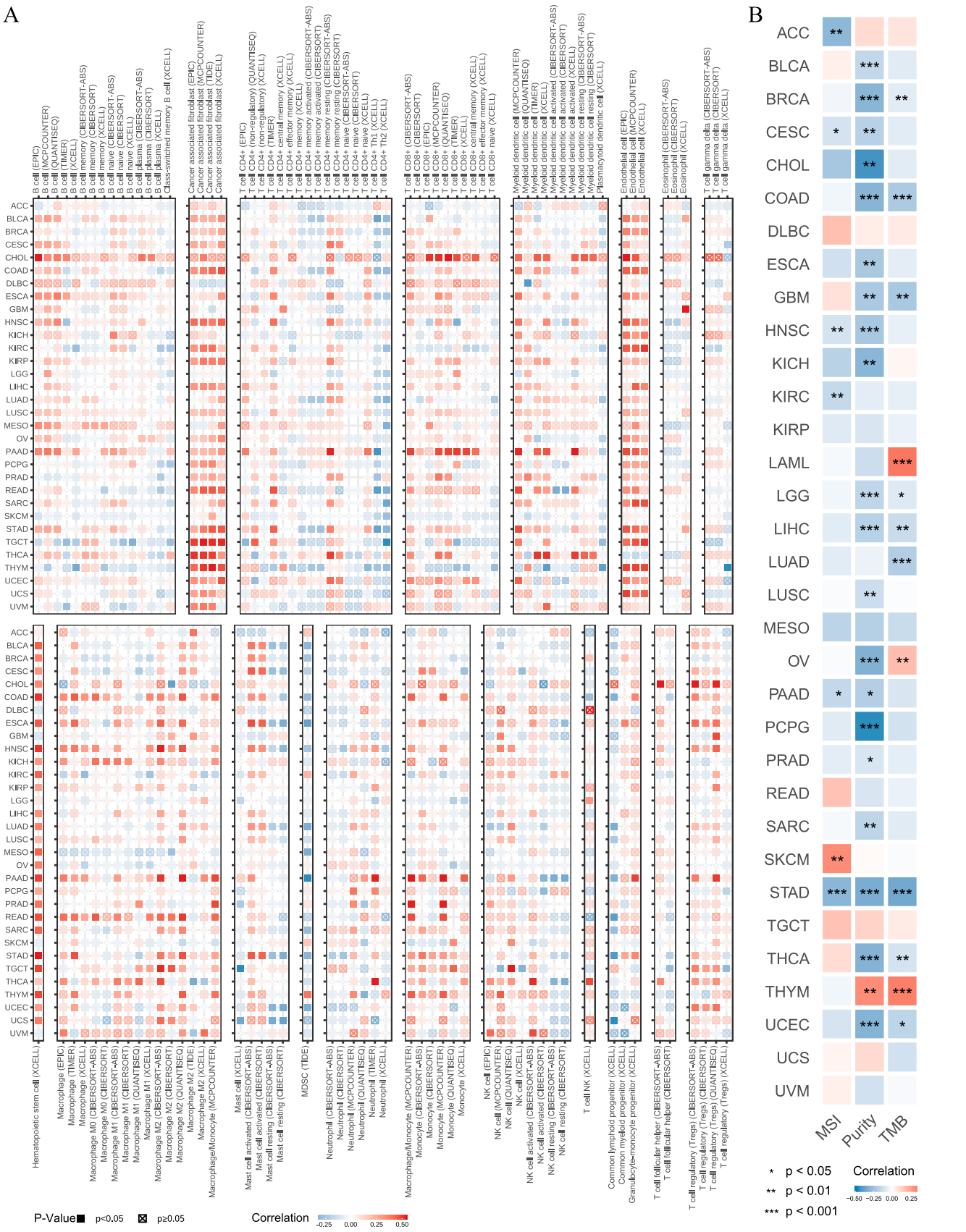

Fig. 2. The pan-cancer analyses of APOD. (A) Spearman's correlation analyses between the expression of APOD and 19 types of immune cells in pan-cancer. (B) Spearman's correlation analyses between the expression of APOD and MSI, purity, and TMB in pan-cancer.

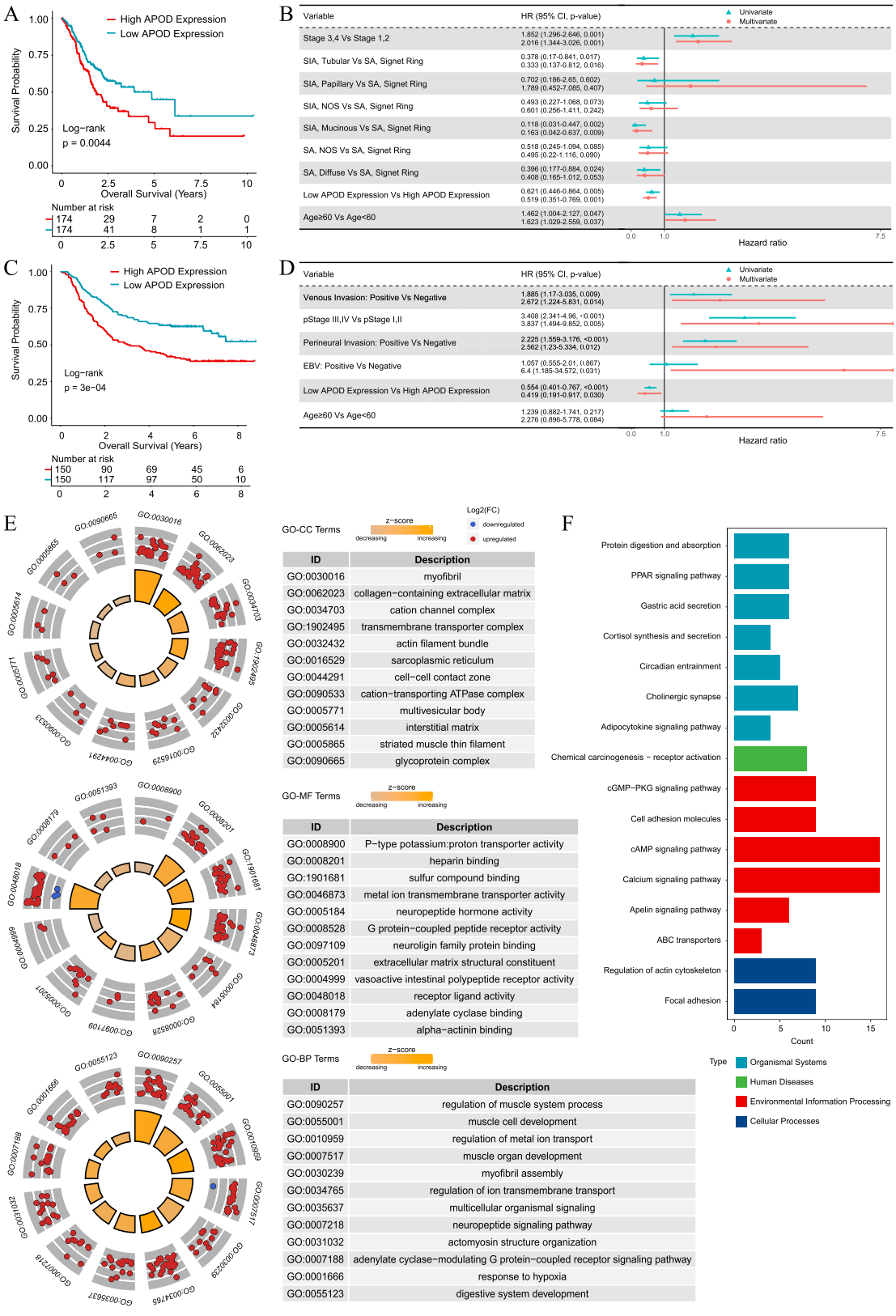

ID	Description
GO:0030016	myofibril
GO:0062023	collagen−containing extracellular matrix
GO:0034703	cation channel complex
GO:1902495	transmembrane transporter complex
GO:0032432	actin filament bundle
GO:0016529	sarcoplasmic reticulum
GO:0044291	cell−cell contact zone
GO:0090533	cation−transporting ATPase complex
GO:0005771	multivesicular body
GO:0005614	interstitial matrix
GO:0005865	striated muscle thin filament
GO:0090665	glycoprotein complex

ID	Description
GO:0008900	P−type potassium:proton transporter activity
GO:0008201	heparin binding
GO:1901681	sulfur compound binding
GO:0046873	metal ion transmembrane transporter activity
GO:0005184	neuropeptide hormone activity
GO:0008528	G protein−coupled peptide receptor activity
GO:0097109	neuroligin family protein binding
GO:0005201	extracellular matrix structural constituent
GO:0004999	vasoactive intestinal polypeptide receptor activity
GO:0048018	receptor ligand activity
GO:0008179	adenylate cyclase binding
GO:0051393	alpha−actinin binding

ID	Description
GO:0090257	regulation of muscle system process
GO:0055001	muscle cell development
GO:0010959	regulation of metal ion transport
GO:0007517	muscle organ development
GO:0030239	myofibril assembly
GO:0034765	regulation of ion transmembrane transport
GO:0035637	multicellular organismal signaling
GO:0007218	neuropeptide signaling pathway
GO:0031032	actomyosin structure organization
GO:0007188	adenylate cyclase−modulating G protein−coupled receptor signaling pathway
GO:0001666	response to hypoxia
GO:0055123	digestive system development

Fig. 3. The prognostic features and functional enrichment analyses of APOD in GC. (A) KM curves for high and low APOD expression groups in TCGA-STAD; (B) Univariate and multivariate CoxPHs were used to calculate the HR values of APOD expression levels and other clinicopathologic indicators in TCGA-STAD. (SIA, Stomach, Intestinal Adenocarcinoma; SA, Stomach, Adenocarcinoma; NOS, Not Otherwise Specified); (C) KM curves for high and low APOD expression groups in GSE62254. (D) Univariate and multivariate CoxPHs were used to calculate the HR values of APOD expression levels and other clinicopathologic indicators in GSE62254; (E) GO analysis was employed for functional enrichment analysis in TCGA-STAD using CC, MF, and BP categories. (F) KEGG database was used for functional enrichment analysis in TCGA-STAD with the results classified into four categories.

development. We then analyzed the association between APOD expression and GC TME using multiple algorithms. CIBERSORT analyses revealed the proportions of immune cells in GC (Supplementary Figure 6B, C), and the high APOD expression group showed lower levels of T cells CD4 memory activated, T cells follicular helper and Mast cells activated (Supplementary Figure 6D, E). ESTIMATE analyses indicated that the high APOD expression group was more likely to have higher stromal score, immune score and ESTIMATE score (Supplementary Figure 7 A, B). We also used the ConsensusTME method, and the results showed higher scores of B cells, endothelial cells, fibroblasts and plasma cells in the high APOD expression group (Supplementary Figure 7 C, D).

3.6. Significant correlations of APOD with multiple cancer biomarkers in GC

Biomarkers can serve as indicators for the onset and progression of diseases, and serve as references for risk stratification and targeted therapy by clinicians. Therefore, we curated gene signatures related to IFN-γ signature, onco-pathways, metabolism pathways and cancer hallmark pathways, and conducted ssGSEA to explore the associations of APOD expression with these biomarkers in GC. Our analyses revealed that the high APOD expression group had lower scores in Interferon-γ, G2M checkpoint, P53 pathway, and higher scores in Metabolism, Apical junction, Myogenesis (Fig. 4A). Scatter plots and violin plots were used to illustrate the correlations of APOD expression with all the biomarkers we collected in GC (Supplementary Figure 8–21).

3.7. High APOD expression in GC indicates lower TMB and poorer immune therapeutic response

In order to evaluate the relationship between APOD expression and immune therapeutic response, a comparison between the gene mutations of high and low APOD expression groups were conducted (Fig. 4B & Supplementary Figure 22 A). Furthermore, based on the grouping of APOD expression levels, we found that patients with high APOD expression had a significantly lower TMB, suggesting that they might have a reduced likelihood of benefiting from immune therapy (Fig. 4C). This finding was supported by the analysis using the TIDE database, which showed that GC patients with high APOD expression had higher TIDE scores, indicating a poorer response to immune therapy compared to those with low APOD expression (Fig. 4D, E). In our analysis of metastatic GC patients treated with pembrolizumab, we observed elevated APOD expression levels in patients who did not respond to immunotherapy (Supplementary Figure 22B), suggesting a potential association between high APOD expression and decreased responsiveness to PD-1 inhibitor therapy.

3.8. High APOD expression in fibroblasts in GC tissues

To investigate the expression patterns of APOD in different cell clusters within GC tissues, we performed analyses using the TISCH2 database on two single-cell datasets, GSE134520 and GSE167297. The results showed that APOD was predominantly expressed in the population of fibroblasts within GC tissues in both cohorts (Fig. 5A-D & Supplementary Figure 23 A, B). The interactions among different cell clusters were shown in heatmaps (Supplementary Figure 23 C, D). Additionally, we performed staining for the fibroblast marker α-SMA and confirmed the expression of APOD in GC fibroblasts (Supplementary Figure 23E-M).

3.9. Interactions between APOD and other proteins

By searching the ComPPI database and calculating interaction scores, we identified additional proteins associated with APOD protein across six types of targets: cytosol, secretory-pathway, extracellular, membrane, mitochondrion, and nucleus, which were represented in an association network (Supplementary Figure 24).

3.10. Identification of potential anti-gc drugs based on APOD expression

We performed drug screening using the NCI-60 cancer cell line panel in the CellMiner database, and the results indicated that APOD expression was negatively correlated with the activity levels of BMS-690514, umbralisib, and others, while positively correlated with PD-98059, Refametinib, and others (Fig. 6A). Analyses through the GDSC database revealed that APOD expression was negatively correlated with the IC50 values of PFI-1, XMD11–85 h, and others, while positively correlated with the IC50 values of rTRAIL, Methotrexate, and others (Fig. 6B, C).

3.11. Immunohistochemical (IHC) staining confirms that high APOD expression is an independent prognostic factor for GC patients

To further support our conclusion, we collected 108 human GC samples along with corresponding clinicopathologic information, forming the ZN-GC cohort. We conducted IHC staining on the tissue microarray (Fig. 7A) and estimated the protein levels of APOD. Chi-square analysis revealed clinicopathological information of the patients in ZN-GC (Supplementary Table 7). KM curves indicated that patients with elevated APOD expression had worse OS (Fig. 7B & Supplementary Figure 5 F), a finding confirmed by RMST analysis (Supplementary Table 8). Univariate and multivariate CoxPHs demonstrated that high APOD expression was an independent prognostic risk factor for GC patients (Fig. 7C). Then we found the model incorporating APOD groups achieved a higher C-index compared to the model without it, suggesting that APOD expression improves the predictive performance of the model and APOD played a significant role in GC prognosis (Supplementary Figure 5 C).

4. Discussion

GC is a prevalent and fatal malignancy with limited treatment options for advanced stages [1, 3, 4]. While anti-PD-L1 and PD-1 inhibitors have shown promise in various cancers, their efficacy in GC remains limited [46,47]. This underscores the urgent need for novel therapeutic targets.

Dysregulated lipid metabolism is a recognized feature of cancer, with tumor cells often relying on it for energy, survival, proliferation, and metastasis [48]. APOs play a crucial role in lipid metabolism and influence various cancer-related processes, making them promising therapeutic targets and biomarkers [7,49]. Among APOs, APOD is recognized as a multi-ligand, multifunctional protein involved in lipid transport, inflammation, and various cancers GC [10]. Its complex regulation suggests potential involvement in multiple biological processes [50–53].

We conducted a comprehensive analysis of APOD in GC using bioinformatics and experimental approaches. Pan-cancer analyses revealed that APOD expression was differentially regulated and correlated with prognosis, immune infiltration, and CNV. We also established a protein-protein interaction network for APOs, highlighting their interconnected roles.

Specifically in GC, APOD expression was negatively correlated with MSI, purity, and TMB, suggesting its potential as a prognostic and immunotherapy response biomarker. High APOD expression was associated with poor prognosis, lower IFN-γ scores, higher metabolic scores, and potentially poorer response to immunotherapy. Single-cell analyses and IHC staining further confirmed high APOD expression in fibroblasts, known to promote tumor progression and immune evasion [54,55], within the GC microenvironment. In addition to utilizing publicly available datasets of GC samples, we also collected 108 tissue samples of GC patients to construct a tissue microarray. By employing IHC staining and corresponding survival analyses, we confirmed that high APOD

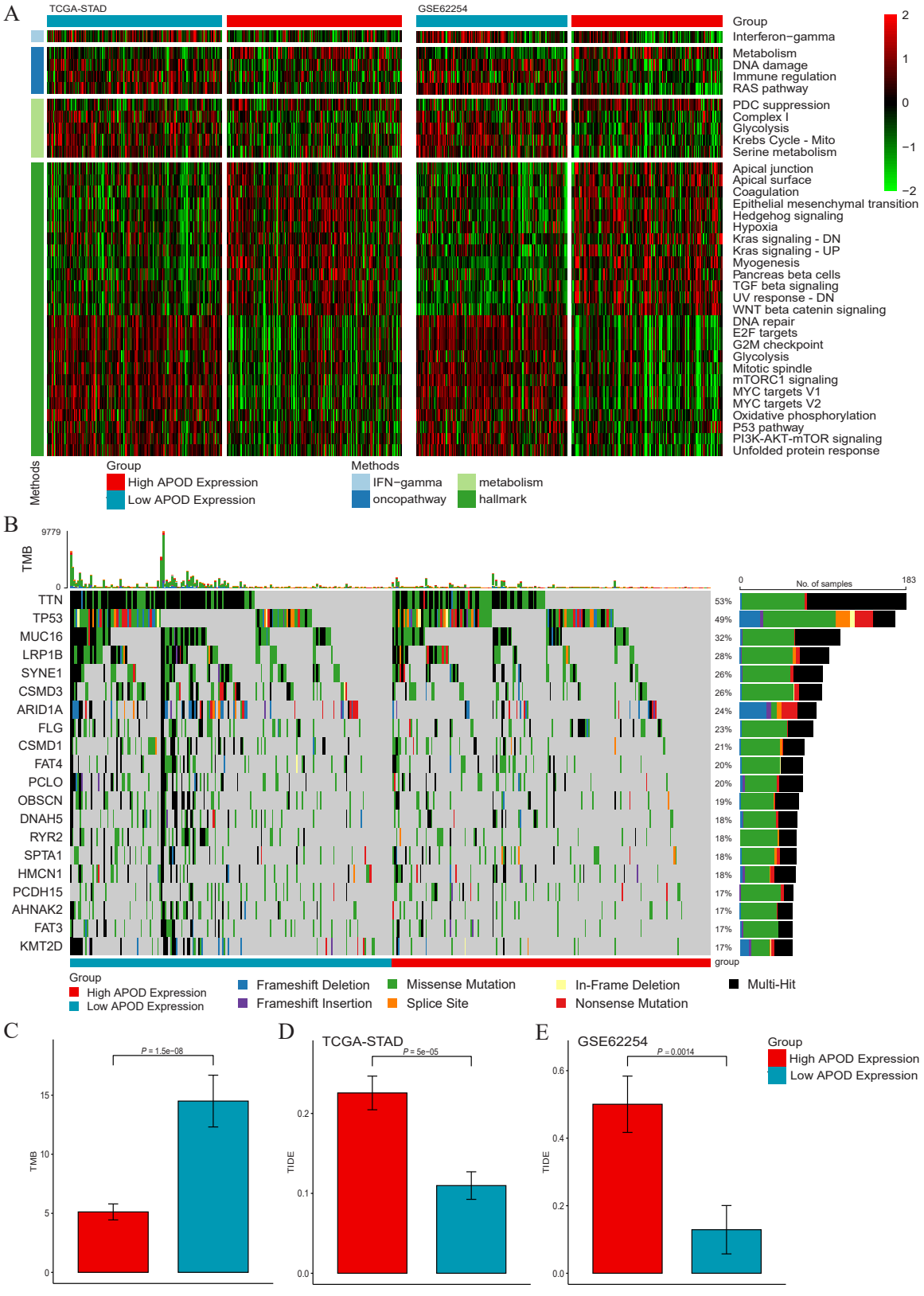

Fig. 4. The correlations between APOD expression and cancer biomarkers, TMB, and immunotherapy efficacy in GC. (A) Heatmap of scores for four types of cancer biomarkers in TCGA-STAD and GSE62254, with samples divided into two groups based on the median expression level of APOD. (B) Mutation landscape of TCGA-STAD, where samples were divided into two groups based on the median expression level of APOD. (C) Comparison of TMB between high and low APOD expression groups. (D) Comparison of TIDE scores between high and low APOD expression groups in TCGA-STAD. (E) Comparison of TIDE scores between high and low APOD expression groups in GSE62254.

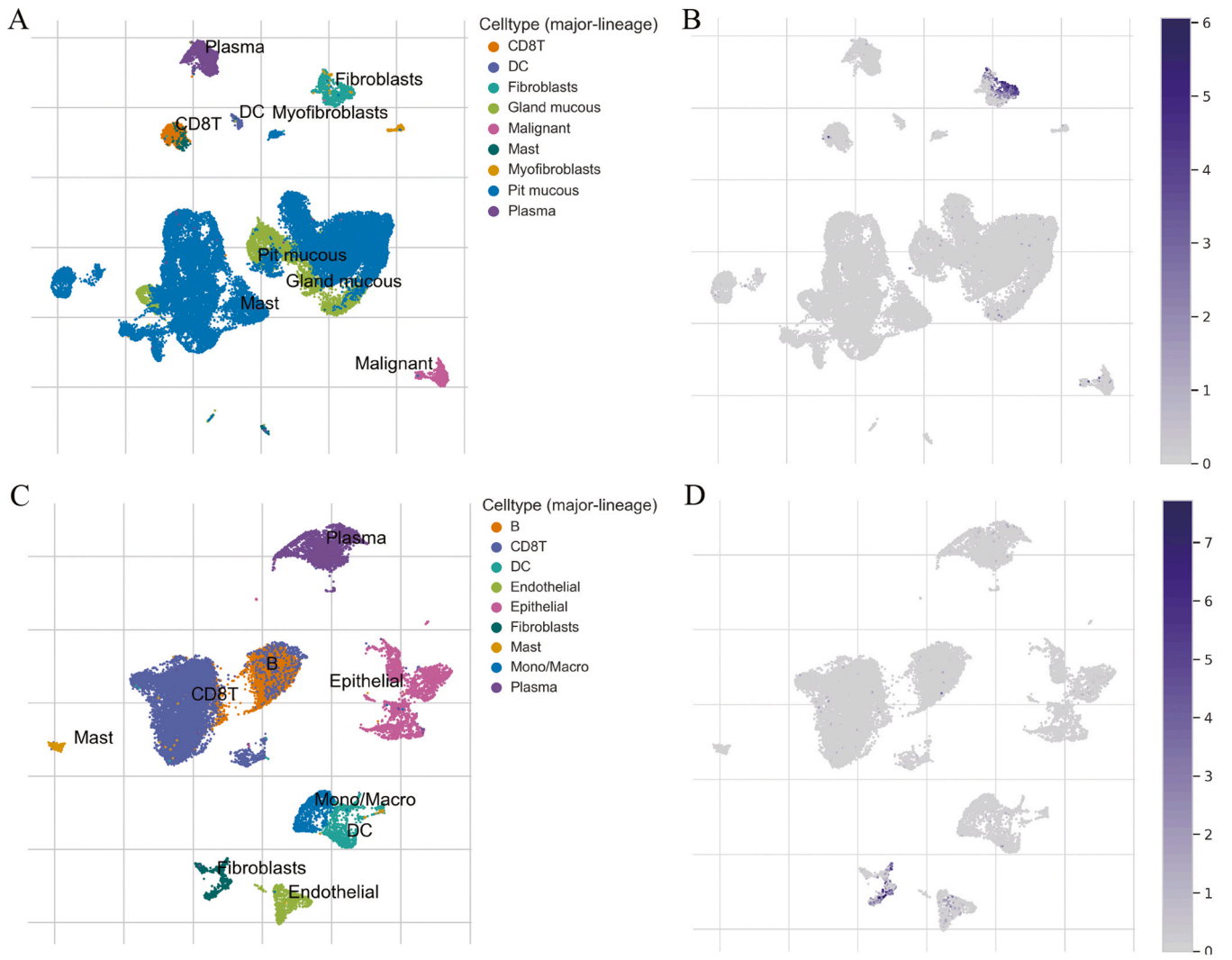

Fig. 5. The expression characteristics of APOD at the single-cell level. (A) Single-cell clustering for GSE134520. (B) Single-cell expression profiles of APOD in cell clusters for GSE134520. (C) Single-cell clustering from GSE167297. (D) Single-cell expression profiles of APOD in cell clusters from GSE167297.

expression was an independent prognostic risk factor for GC patients.

Our findings revealed that APOD was downregulated in GC tissues compared to adjacent normal tissues. Analyses suggested that high expression of APOD served as an independent risk prognostic factor for GC. While numerous studies have demonstrated a correlation between elevated expression of certain genes in tumors and a poorer prognosis, it is essential to note that this is not universally applicable. For example, previous study found that CHAC1 was downregulated compared to normal samples, while upregulation of CHAC1 expression was identified as an independent risk factor for poor prognosis in these patients [56]. Therefore, the low expression of APOD in GC tumors is not contradictory to its role as an unfavorable prognostic factor.

Multiple studies have revealed a positive association between MSI and enhanced survival rates in GC [18, 57, 58]. The hypermutated trait of MSI tumors results in the prolific expression of diverse peptides with potential to function as neoantigens. These neopeptides trigger robust recruitment and activation of T-cells [59], a phenomenon potentially contributing to the favorable response to immunotherapy observed in MSI-high GC patients [60–62]. This enhanced immune recognition is mirrored by the association between high TMB and improved clinical response to immunotherapy [63], and several studies have suggested that GC patients with high TMB may have a better prognosis [64–66]. Therefore, the significant negative correlation between APOD expression and both MSI and TMB in GC suggested its potential as a biomarker for predicting immunotherapy response and patient prognosis, informing crucial clinical treatment decisions. Furthermore, we found that patients with high APOD expression had higher TIDE scores and metastatic GC patients who responded to pembrolizumab treatment had lower APOD expression. These findings suggested that high APOD expression might be associated with a poorer response to immunotherapy.

The TME is a bustling neighborhood surrounding tumors, inhabited by diverse non-cancer cells such as immune sentinels, supportive fibroblasts, and blood vessel builders. These cellular cohabitants are increasingly recognized as potent forces shaping cancer growth and development [67]. We found that APOD expression was negatively correlated with tumor purity and showed significant associations with multiple components within different TME scoring algorithms. Further investigation into this relationship, our single-cell analysis and IHC staining showed that APOD was expressed not only in GC tumor cells but also in fibroblasts within the TME. Fibroblasts are a predominant cell type within the TME and are responsible for the majority of extracellular components within the tumor, such as extracellular matrix and soluble factors. When quiescent fibroblasts switch to CAFs, they induce a variety of pro-tumorigenic processes, including remodeling of tissue architecture and suppression of the local immune response [54,55]. CAFs have been found to have diverse functions, including matrix deposition and remodeling, extensive reciprocal signaling interactions with cancer

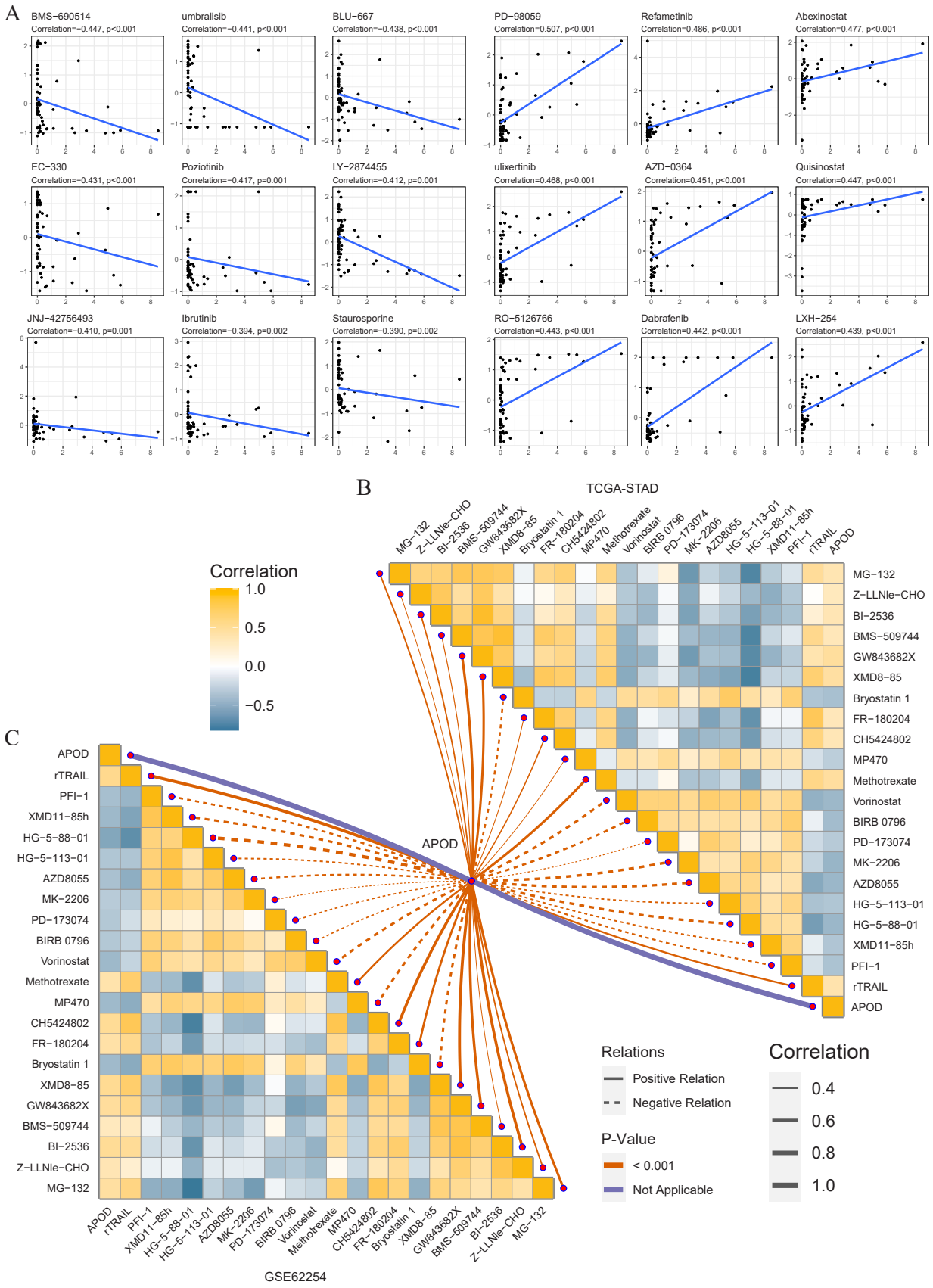

Fig. 6. Screening anti-GC drugs based on APOD expression. (A) Spearman's correlations between APOD expression and drugs in the CellMiner database. (B) Spearman's correlations between APOD expression and drug IC50 values in TCGA-STAD. (C) and Spearman's correlations between APOD expression and drug IC50 values in GSE62254.

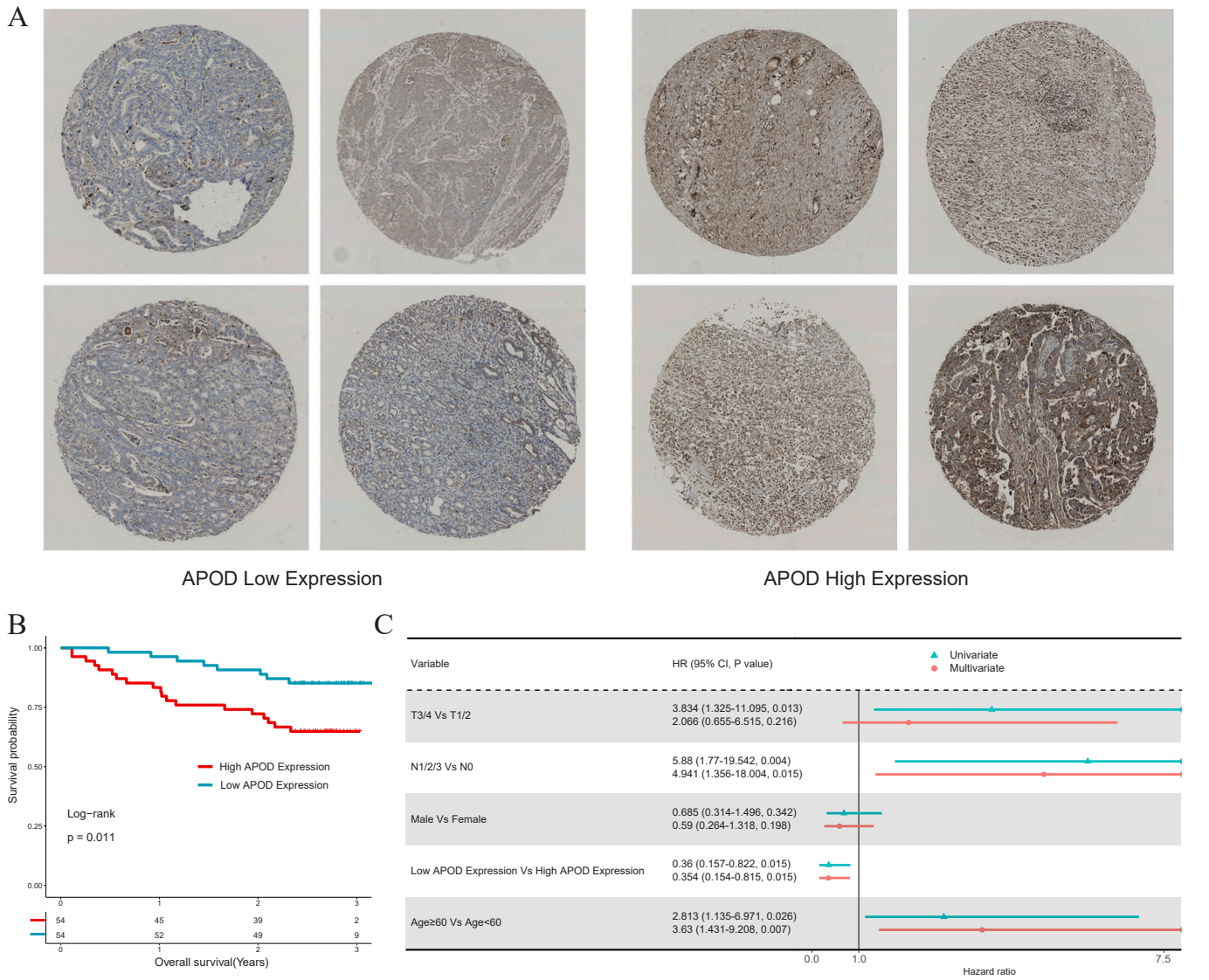

Fig. 7. Independent validation of the prognostic roles of APOD in GC. (A) Representative IHC staining images in high and low APOD expression groups. (B) KM curves for high and low APOD expression groups in ZN-GC. (C) Univariate and multivariate CoxPHs of APOD expression levels and other clinicopathological indicators in ZN-GC, where T represents T stages and N represents N stages.

cells, and crosstalk with infiltrating immune cells [68]. They also play a pivotal role in tumor progression, therapeutic resistance, and immune evasion through secretion of effective molecules and remodeling of the extracellular matrix [69]. This may partly explain why high APOD expression was associated with poorer prognosis and worse response to immunotherapy.

Our study has several limitations. Further experimental evidence is required to elucidate the mechanisms by which APOD functions in GC. Moreover, to further validate the efficacy of the anti-GC drugs identified in our study, additional cellular and animal experiments are needed.

Overall, our study uncovers the potential of APOD as a valuable prognostic, therapeutic, and immune response biomarker in GC. Further research is warranted to fully translate these findings into clinical applications for improved GC management.

5. Conclusions

In conclusion, by comprehensively analyzing the pan-cancer features of APOs, with a specific focus on APOD in GC, our study has identified APOD as a potentially promising therapeutic target. We found a significant association between high APOD expression and worse prognosis in GC patients. Moreover, APOD was associated with TME and multiple cancer biomarkers in GC. Notably, high APOD expression in GC patients was correlated with lower TMB and MSI, suggesting a decreased response to immunotherapy. Additionally, potential anti-GC drugs were identified based on APOD expression, providing valuable insights into alternative therapeutic options. Overall, our study not only sheds light on the critical roles of APOD in GC progression but also underscores its potential as a therapeutic target, paving the way for the development of personalized medicine approaches for GC patients.

Ethics approval and consent to participate

The collection of tissues for construction of the ZN-GC cohort was approved by the Institutional Review Board of Zhongnan Hospital of Wuhan University (2020133) and was under a waiver of informed consent from the participants.

Consent for publication

Not applicable.

Funding

This research received no external funding.

Declaration of Competing Interest

All authors declare no conflict of interest.

Acknowledgments

Not applicable.

Appendix A. Supporting information

Supplementary data associated with this article can be found in the online version at doi:10.1016/j.csbj.2024.02.015.

References

[1] Smyth EC, Nilsson M, Grabsch HI, van Grieken NC, Lordick F. Gastric cancer. Lancet 2020;396(10251):635–48.
[2] Zhang XY, Zhang PY. Gastric cancer: somatic genetics as a guide to therapy. J Med Genet 2017;54(5):305–12.
[3] Johnston FM, Beckman M. Updates on management of gastric cancer. Curr Oncol Rep 2019;21(8):67.
[4] Digklia A, Wagner AD. Advanced gastric cancer: current treatment landscape and future perspectives. World J Gastroenterol 2016;22(8):2403–14.
[5] Soon WW, Hariharan M, Snyder MP. High-throughput sequencing for biology and medicine. Mol Syst Biol 2013;9:640.
[6] Rego SM, Snyder MP. High throughput sequencing and assessing disease risk. Cold Spring Harb Perspect Med 2019;9(1).
[7] Ren L, Yi J, Li W, Zheng X, Liu J, Wang J, et al. Apolipoproteins and cancer. Cancer Med 2019;8(16):7032–43.
[8] Ma MZ, Yuan SQ, Chen YM, Zhou ZW. Preoperative apolipoprotein B/apolipoprotein A1 ratio: a novel prognostic factor for gastric cancer. OncoTargets Ther 2018;11:2169–76.
[9] Zheng P, Luo Q, Wang W, Li J, Wang T, Wang P, et al. Tumor-associated macrophages-derived exosomes promote the migration of gastric cancer cells by transfer of functional Apolipoprotein E. Cell Death Dis 2018;9(4):434.
[10] Rassart E, Desmarais F, Najyb O, Bergeron KF, Mounier C. Apolipoprotein D. Gene 2020;756:144874.
[11] Jankovic-Karasoulos T, Bianco-Miotto T, Butler MS, Butler LM, McNeil CM, O'Toole SA, et al. Elevated levels of tumour apolipoprotein D independently predict poor outcome in breast cancer patients. Histopathology 2020;76(7):976–87.
[12] Utsunomiya T, Ogawa K, Yoshinaga K, Ohta M, Yamashita K, Mimori K, et al. Clinicopathologic and prognostic values of apolipoprotein D alterations in hepatocellular carcinoma. Int J Cancer 2005;116(1):105–9.
[13] Ogawa K, Utsunomiya T, Mimori K, Yamashita K, Okamoto M, Tanaka F, et al. Genomic screens for genes upregulated by demethylation in colorectal cancer: possible usefulness for clinical application. Int J Oncol 2005;27(2):417–26.
[14] Miranda E, Vizoso F, Martin A, Quintela I, Corte MD, Segui ME, et al. Apolipoprotein D expression in cutaneous malignant melanoma. J Surg Oncol 2003;83(2):99–105.
[15] Goldman MJ, Craft B, Hastie M, Repecka K, McDade F, Kamath A, et al. Visualizing and interpreting cancer genomics data via the Xena platform. Nat Biotechnol 2020;38(6):675–8.
[16] Ellrott K, Bailey MH, Saksena G, Covington KR, Kandoth C, Stewart C, et al. Scalable open science approach for mutation calling of tumor exomes using multiple genomic pipelines. Cell Syst 2018;6(3):271–81. e7.
[17] Cancer Genome Atlas Research N. Comprehensive molecular characterization of gastric adenocarcinoma. Nature 2014;513(7517):202–9.
[18] Cristescu R, Lee J, Nebozhyn M, Kim KM, Ting JC, Wong SS, et al. Molecular analysis of gastric cancer identifies subtypes associated with distinct clinical outcomes. Nat Med 2015;21(5):449–56.
[19] Liu X., Wang Z., Shi H., Li S., Wang X. CBioProfiler: a web and standalone pipeline for cancer biomarker and subtype characterization. medRxiv. 2024: 2022.01.17.22269448.
[20] Liu CJ, Hu FF, Xie GY, Miao YR, Li XW, Zeng Y, et al. GSCA: an integrated platform for gene set cancer analysis at genomic, pharmacogenomic and immunogenomic levels. Brief Bioinform 2023;24(1).
[21] Liu J, Lichtenberg T, Hoadley KA, Poisson LM, Lazar AJ, Cherniack AD, et al. An integrated TCGA pan-cancer clinical data resource to drive high-quality survival outcome analytics. Cell 2018;173(2):400–16. e11.
[22] Beroukhim R, Mermel CH, Porter D, Wei G, Raychaudhuri S, Donovan J, et al. The landscape of somatic copy-number alteration across human cancers. Nature 2010;463(7283):899–905.
[23] Mayakonda A, Lin DC, Assenov Y, Plass C, Koeffler HP. Maftools: efficient and comprehensive analysis of somatic variants in cancer. Genome Res 2018;28(11):1747–56.
[24] Li T, Fu J, Zeng Z, Cohen D, Li J, Chen Q, et al. TIMER2.0 for analysis of tumor-infiltrating immune cells. Nucleic Acids Res 2020;48(W1). W509-W14.
[25] Bonneville R, Krook MA, Kautto EA, Miya J, Wing MR, Chen HZ, et al. Landscape of Microsatellite Instability Across 39 Cancer Types. JCO Precis Oncol 2017;2017.
[26] Thorsson V, Gibbs DL, Brown SD, Wolf D, Bortone DS, Ou Yang TH, et al. The immune landscape of cancer. Immunity 2018;48(4):812–30. e14.
[27] Ru B, Wong CN, Tong Y, Zhong JY, Zhong SSW, Wu WC, et al. TISIDB: an integrated repository portal for tumor-immune system interactions. Bioinformatics 2019;35(20):4200–2.
[28] Shen W, Song Z, Zhong X, Huang M, Shen D, Gao P, et al. Sangerbox: a comprehensive, interaction-friendly clinical bioinformatics analysis platform. iMeta 2022;1(3). e36.
[29] Yoshihara K, Shahmoradgoli M, Martinez E, Vegesna R, Kim H, Torres-Garcia W, et al. Inferring tumour purity and stromal and immune cell admixture from expression data. Nat Commun 2013;4:2612.
[30] Newman AM, Liu CL, Green MR, Gentles AJ, Feng W, Xu Y, et al. Robust enumeration of cell subsets from tissue expression profiles. Nat Methods 2015;12(5):453–7.
[31] Jimenez-Sanchez A, Cast O, Miller ML. Comprehensive benchmarking and integration of tumor microenvironment cell estimation methods. Cancer Res 2019;79(24):6238–46.
[32] Heimes AS, Hartner F, Almstedt K, Krajnak S, Lebrecht A, Battista MJ, et al. Prognostic significance of interferon-gamma and its signaling pathway in early breast cancer depends on the molecular subtypes. Int J Mol Sci 2020;21(19).
[33] Davoli T, Uno H, Wooten EC, Elledge SJ. Tumor aneuploidy correlates with markers of immune evasion and with reduced response to immunotherapy. Science 2017;355(6322).
[34] Ricketts CJ, De Cubas AA, Fan H, Smith CC, Lang M, Reznik E, et al. The cancer genome atlas comprehensive molecular characterization of renal cell carcinoma. Cell Rep 2018;23(1):313–26. e5.
[35] Liberzon A, Birger C, Thorvaldsdottir H, Ghandi M, Mesirov JP, Tamayo P. The molecular signatures database (MSigDB) hallmark gene set collection. Cell Syst 2015;1(6):417–25.
[36] Liu G, Yang Y, Kang X, Xu H, Ai J, Cao M, et al. A pan-cancer analysis of lipid metabolic alterations in primary and metastatic cancers. Sci Rep 2023;13(1):13810.
[37] Jiang P, Gu S, Pan D, Fu J, Sahu A, Hu X, et al. Signatures of T cell dysfunction and exclusion predict cancer immunotherapy response. Nat Med 2018;24(10):1550–8.
[38] Kim ST, Cristescu R, Bass AJ, Kim KM, Odegaard JI, Kim K, et al. Comprehensive molecular characterization of clinical responses to PD-1 inhibition in metastatic gastric cancer. Nat Med 2018;24(9):1449–58.
[39] Sun D, Wang J, Han Y, Dong X, Ge J, Zheng R, et al. TISCH: a comprehensive web resource enabling interactive single-cell transcriptome visualization of tumor microenvironment. Nucleic Acids Res 2021;49(D1). D1420-D30.
[40] Zhang P, Yang M, Zhang Y, Xiao S, Lai X, Tan A, et al. Dissecting the single-cell transcriptome network underlying gastric premalignant lesions and early gastric cancer. Cell Rep 2019;27(6):1934–47. e5.
[41] Jeong HY, Ham IH, Lee SH, Ryu D, Son SY, Han SU, et al. Spatially distinct reprogramming of the tumor microenvironment based on tumor invasion in diffuse-type gastric cancers. Clin Cancer Res 2021;27(23):6529–42.
[42] Reinhold WC, Sunshine M, Liu H, Varma S, Kohn KW, Morris J, et al. CellMiner: a web-based suite of genomic and pharmacologic tools to explore transcript and drug patterns in the NCI-60 cell line set. Cancer Res 2012;72(14):3499–511.
[43] Geeleher P, Cox N, Huang RS. pRRophetic: an R package for prediction of clinical chemotherapeutic response from tumor gene expression levels. PLOS One 2014;9(9):e107468.
[44] Veres DV, Gyurko DM, Thaler B, Szalay KZ, Fazekas D, Korcsmaros T, et al. ComPPI: a cellular compartment-specific database for protein-protein interaction network analysis. Nucleic Acids Res 2015;43(Database issue). D485-93.
[45] Bankhead P, Loughrey MB, Fernandez JA, Dombrowski Y, McArt DG, Dunne PD, et al. QuPath: open source software for digital pathology image analysis. Sci Rep 2017;7(1):16878.
[46] Bang YJ, Ruiz EY, Van Cutsem E, Lee KW, Wyrwicz L, Schenker M, et al. Phase III, randomised trial of avelumab versus physician's choice of chemotherapy as third-line treatment of patients with advanced gastric or gastro-oesophageal junction cancer: primary analysis of JAVELIN gastric 300. Ann Oncol 2018;29(10):2052–60.
[47] Kang YK, Boku N, Satoh T, Ryu MH, Chao Y, Kato K, et al. Nivolumab in patients with advanced gastric or gastro-oesophageal junction cancer refractory to, or intolerant of, at least two previous chemotherapy regimens (ONO-4538-12, ATTRACTION-2): a randomised, double-blind, placebo-controlled, phase 3 trial. Lancet 2017;390(10111):2461–71.
[48] Bian X, Liu R, Meng Y, Xing D, Xu D, Lu Z. Lipid metabolism and cancer. J Exp Med 2021;218(1).
[49] Broadfield LA, Pane AA, Talebi A, Swinnen JV, Fendt SM. Lipid metabolism in cancer: new perspectives and emerging mechanisms. Dev Cell 2021;56(10):1363–93.
[50] Lambert J, Provost PR, Marcel YL, Rassart E. Structure of the human apolipoprotein D gene promoter region. Biochim Biophys Acta 1993;1172(1-2):190–2.
[51] Do Carmo S, Seguin D, Milne R, Rassart E. Modulation of apolipoprotein D and apolipoprotein E mRNA expression by growth arrest and identification of key elements in the promoter. J Biol Chem 2002;277(7):5514–23.
[52] Hummasti S, Laffitte BA, Watson MA, Galardi C, Chao LC, Ramamurthy L, et al. Liver X receptors are regulators of adipocyte gene expression but not differentiation: identification of apoD as a direct target. J Lipid Res 2004;45(4):616–25.

[53] Do Carmo S., Levros L.C., Jr., Rassart E. Modulation of apolipoprotein D expression and translocation under specific stress conditions. Biochim Biophys Acta. 2007; 1773(6):954–969.
[54] Chen X, Song E. Turning foes to friends: targeting cancer-associated fibroblasts. Nat Rev Drug Discov 2019;18(2):99–115.
[55] Biffi G, Tuveson DA. Diversity and biology of cancer-associated fibroblasts. Physiol Rev 2021;101(1):147–76.
[56] Li D, Liu S, Xu J, Chen L, Xu C, Chen F, et al. Ferroptosis-related gene CHAC1 is a valid indicator for the poor prognosis of kidney renal clear cell carcinoma. J Cell Mol Med 2021;25(7):3610–21.
[57] Miceli R, An J, Di Bartolomeo M, Morano F, Kim ST, Park SH, et al. Prognostic impact of microsatellite instability in asian gastric cancer patients enrolled in the ARTIST trial. Oncology 2019;97(1):38–43.
[58] Pietrantonio F, Miceli R, Raimondi A, Kim YW, Kang WK, Langley RE, et al. Individual patient data meta-analysis of the value of microsatellite instability as a biomarker in gastric cancer. J Clin Oncol 2019;37(35):3392–400.
[59] Puliga E, Corso S, Pietrantonio F, Giordano S. Microsatellite instability in gastric cancer: between lights and shadows. Cancer Treat Rev 2021;95:102175.
[60] Janjigian YY, Sanchez-Vega F, Jonsson P, Chatila WK, Hechtman JF, Ku GY, et al. Genetic predictors of response to systemic therapy in esophagogastric cancer. Cancer Discov 2018;8(1):49–58.
[61] Chao J, Fuchs CS, Shitara K, Tabernero J, Muro K, Van Cutsem E, et al. Pembrolizumab (pembro) in microsatellite instability-high (MSI-H) advanced gastric/gastroesophageal junction (G/GEJ) cancer by line of therapy. J Clin Oncol 2020;38(4):430.
[62] Joshi SS, Badgwell BD. Current treatment and recent progress in gastric cancer. CA Cancer J Clin 2021;71(3):264–79.
[63] Wang F, Wei XL, Wang FH, Xu N, Shen L, Dai GH, et al. Safety, efficacy and tumor mutational burden as a biomarker of overall survival benefit in chemo-refractory gastric cancer treated with toripalimab, a PD-1 antibody in phase Ib/II clinical trial NCT02915432. Ann Oncol 2019;30(9):1479–86.
[64] Kim HD, Ryu MH, Park YS, Lee SY, Moon M, Kang YK. Insertion-deletion rate is a qualitative aspect of the tumor mutation burden associated with the clinical outcomes of gastric cancer patients treated with nivolumab. Gastric Cancer 2022; 25(1):226–34.
[65] Shah MA, Cunningham D, Metges JP, Van Cutsem E, Wainberg Z, Elboudwarej E, et al. Randomized, open-label, phase 2 study of andecaliximab plus nivolumab versus nivolumab alone in advanced gastric cancer identifies biomarkers associated with survival. J Immunother Cancer 2021;9(12).
[66] Cheng Y, Bu D, Zhang Q, Sun R, Lyle S, Zhao G, et al. Genomic and transcriptomic profiling indicates the prognosis significance of mutational signature for TMB-high subtype in Chinese patients with gastric cancer. J Adv Res 2022.
[67] Aran D, Sirota M, Butte AJ. Systematic pan-cancer analysis of tumour purity. Nat Commun 2015;6:8971.
[68] Sahai E, Astsaturov I, Cukierman E, DeNardo DG, Egeblad M, Evans RM, et al. A framework for advancing our understanding of cancer-associated fibroblasts. Nat Rev Cancer 2020;20(3):174–86.
[69] Xu Y, Li W, Lin S, Liu B, Wu P, Li L. Fibroblast diversity and plasticity in the tumor microenvironment: roles in immunity and relevant therapies. Cell Commun Signal 2023;21(1):234.